Journal of Alloys and Compounds 509 (2011) 3148–3154

Contents lists available at ScienceDirect

Journal of Alloys and Compounds

journal homepage: www.elsevier.com/locate/jallcom

Effect of potassium concentration on the structure and electrical properties of lead-free $Bi_{0.5}$ $(Na,K)_{0.5}$ TiO_3–$BiAlO_3$ piezoelectric ceramics

Aman Ullah [a], Chang Won Ahn [b], Ali Hussain [a], Sun Young Lee [a], Jin Soo Kim [a], Ill Won Kim [a,*]

[a] Department of Physics, University of Ulsan, Ulsan 680-749, South Korea
[b] Convergence Components R&D Division, KETI, Seongnam 463-816, South Korea

ARTICLE INFO

Article history:
Received 27 August 2010
Received in revised form 2 December 2010
Accepted 3 December 2010
Available online 13 December 2010

Keywords:
Ceramics
Sintering
Microstructure
Ferroelectrics
Piezoelectricity

ABSTRACT

In this study, lead-free $0.975[Bi_{0.5}(Na_{1-x}K_x)_{0.5}TiO_3]$–$0.025BiAlO_3$ piezoelectric ceramics (BNKT–BA) with x ranging from 0 to 0.25 were fabricated using a conventional solid state reaction. The effects of potassium concentration (x) on the structure and electrical properties of the ceramics were investigated. The X-ray diffraction patterns revealed that the addition of K^+ improved the crystal symmetry of the BNKT–BA ceramics and produced a rhombohedral–tetragonal morphotropic phase boundary (MPB) in the range of $0.15 \leq x \leq 0.20$. The increase of the K^+ concentration resulted in a decreased grain growth rate and promoted the formation of grains with a cubic shape. The BNKT–BA ceramics exhibited high remanent polarizations of 25 $\mu C/cm^2$ near the rhombohedral side of the MPB composition ($x = 0.15$). The polarization and strain hysteresis loops demonstrated that an increased K^+ concentration ($x \geq 0.20$) destabilized the ferroelectric order of the BNKT–BA ceramics, leading to degradation of the remanent polarization and coercive field. However, the destabilization of the ferroelectric order was accompanied by significant enhancements in the bipolar and unipolar strains. A large electric field-induced strain ($S = 0.33\%$) and a corresponding normalized strain ($d^*_{33} = S_{max}/E_{max} = 533$ pm/V) were obtained on the tetragonal side of the MPB composition ($x = 0.22$).

1. Introduction

Lead oxide-based piezoelectric solid solutions, represented as $Pb(Zr,Ti)O_3$ (PZT), are widely used in piezoelectric actuators, sensors, and transducers due to their high-performance piezoelectric properties [1,2]. However, lead is considered to be toxic and has been barred from many commercial applications. As such, lead-free piezoelectrics have become the focus of intense interest in both industry and academia [3,4].

$Bi_{0.5}Na_{0.5}TiO_3$ (BNT) ceramic with a rhombohedral perovskite structure is considered to be a good candidate for lead-free piezoelectric ceramics because of its strong ferroelectric behavior at room temperature [5]. However, poling of pure BNT ceramic is difficult due to its high conductivity. Furthermore, the piezoelectric properties of BNT ceramic are too low for practical applications. To improve the piezoelectric properties, a number of BNT-based solid solutions such as BNT–$BaTiO_3$ [6,7], BNT–$KNbO_3$ [8], BNT–$(BaSr)TiO_3$ [9], BNT–$SrTiO_3$ [10], BNT–$SrTiO_3$–$Bi_{0.5}Li_{0.5}TiO_3$ [11], BNT–$Bi_{0.5}K_{0.5}TiO_3$ (BNKT) [12–16], BNT–$Bi_{0.5}K_{0.5}TiO_3$–$BiFeO_3$ [17], and BNT–$BaTiO_3$–$BiFeO_3$ [18] have been developed and extensively studied. Among these BNT-based solid solutions, the binary $(1-x)$BNT–xBKT (BNKT) class of materials has received considerable attention due to its excellent ferroelectric and piezoelectric properties near the rhombohedral–tetragonal morphotropic phase boundary (MPB) with $0.16 \leq x \leq 0.20$ [12–14].

Recently, $BiAlO_3$ (BA) has garnered special attention due to its relatively cheap constituting element and excellent ferroelectric properties [19]. Theoretical calculations predict that BA has a rhombohedral perovskite symmetry, a large spontaneous polarization of about ~76 $\mu C/cm^2$, and a high Curie temperature of about ~527 °C [19]. Zylberberg et al. synthesized BA and confirmed that it is indeed ferroelectric and has a Curie temperature (T_c) > 520 °C [20]. However, its poor thermal stability and consequent extreme synthesis conditions have limited its use in its pure form in practical applications [20]. Therefore, attempts have been made to stabilize BA by solid-solutioning with other stable perovskite materials. Watanabe et al. [21] fabricated $(1-x)Bi_{0.5}Na_{0.5}TiO_3$–$xBiAlO_3$ ferroelectric ceramics and evaluated their electrical properties. Yu and Ye [22] added a small amount of $BiAlO_3$ to the $Na_{0.5}Bi_{0.5}TiO_3$ (NBT–BA) ceramics system and reported excellent ferroelectric and piezoelectric properties. Hiruma et al. [23] synthesized $(1-x)(Bi_{1/2}Na_{1/2})TiO_3$–$xBa(Al_{1/2}Nb_{1/2})O_3$ (BNT–BAN) solid solution ceramics and reported a maximum strain of approximately 0.40% and a corresponding normalized strain, d^*_{33}, of

* Corresponding author at: Department of Physics, University of Ulsan, Nam-Ulsan, P.O. Box 18, Nam Gu, Ulsan 680-749, South Korea.
Tel.: +82 52 259 2323; fax: +82 52 259 1693.
E-mail address: kimiw@mail.ulsan.ac.kr (I.W. Kim).

0925-8388/$ – see front matter © 2010 Elsevier B.V. All rights reserved.
doi:10.1016/j.jallcom.2010.12.027

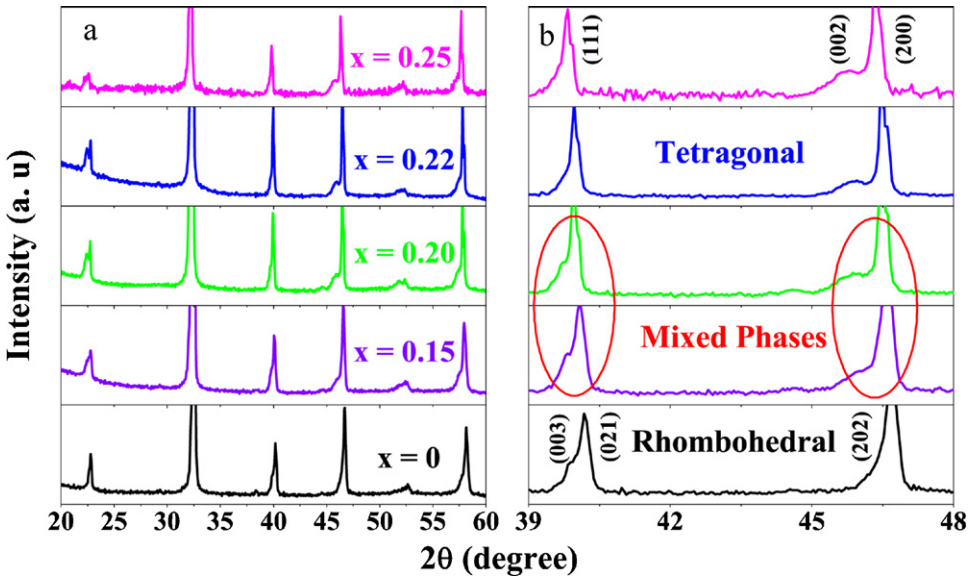

Fig. 1. X-ray diffraction (XRD) patterns of the BNKT–BA ceramics in 2θ ranges of (a) 20–60° and (b) 39–48°.

533 pm/V at $x = 0.055$. Recently, we reported enhanced ferroelectric and piezoelectric properties of $(1-x)Bi_{0.5}Na_{0.5}TiO_3$–$xBiAlO_3$ ceramics [24]. However, our more recent report involving $BiAlO_3$-modified $Bi_{0.5}(Na_{0.75}K_{0.25})_{0.5}TiO_3$ (BNKT25–BA) ceramics resulted in slightly different behavior than that observed with $(1-x)Bi_{0.5}Na_{0.5}TiO_3$–$xBiAlO_3$ [25]. It was found that the ferroelectric order of the $Bi_{0.5}(Na_{0.75}K_{0.25})_{0.5}TiO_3$ ceramics was disrupted significantly by the $BiAlO_3$ addition, which resulted in degradation of the remanent polarization and piezoelectric constant, d_{33}. Instead, a pronounced enhancement in the strain response was observed, which peaked at a $BiAlO_3$ concentration of ~0.025 (2.5 mol%). Hence, the addition of ~2.5 mol% $BiAlO_3$ was chosen for the present study. The observed shift in the electrical properties of $BiAlO_3$-modified BNT and BNKT ceramics [24,25] due to the presence of K^+ content motivated the investigation of the effects of the K^+ concentration on the electrical properties of BNKT–$BiAlO_3$ ceramics. Therefore, in the present study, we investigated the effect of K^+ concentration on the structure and electrical properties of 2.5 mol% $BiAlO_3$-modified $Bi_{0.5}(Na_{1-x}K_x)_{0.5}TiO_3$ (BNKT) ceramics.

2. Experimental

The $0.975[Bi_{0.5}(Na_{1-x}K_x)_{0.5}TiO_3]$–$0.025BiAlO_3$ ($x = 0$, 0.15, 0.20, 0.22, and 0.25) piezoelectric ceramics were synthesized using a conventional solid state reaction method using Bi_2O_3, TiO_2, Al_2O_3 (99.9%, High Purity Chemicals), Na_2CO_3 (99.9%, Cerac Specialty Inorganics), and K_2CO_3 (≥99%, Sigma–Aldrich) as the raw materials. Before weighing, the powders were dried in an oven at 100 °C for 12 h. Each material was weighed according to the stoichiometric formula and ball milled for 24 h in ethanol with zirconia balls. The dried slurries were calcined at 800 °C for 2 h and then ball milled again for 24 h. The powders were pulverized, mixed with an aqueous polyvinyl alcohol (PVA) solution, and pressed into green disks with diameters of 13 mm under a pressure of 100 MPa.

Sintering was carried out at 1150–1170 °C for 2 h in covered alumina crucibles. To prevent the vaporization of Bi, Na, and K, the disks were embedded in a powder of the same composition. The crystal structures of the ceramics were characterized using an X-ray diffractometer (XRD, X'pert PRO MRD, Philips). For microstructural analysis, the surface of the as-sintered samples was removed by lapping. The lapped samples were then thoroughly polished and thermally etched at 1100 °C for 1 h. Finally, scanning electron microscopy (JSM-5610LV) was employed to examine the microstructure of the polished and thermally etched samples. The sintered disks were polished to measure their electrical properties and silver paste was applied to both surfaces of the disks to form an electrode. After applying the silver, the disks were fired at 700 °C for 30 min and the temperature dependences of the dielectric properties were measured using an impedance analyzer (HP4192A). The ferroelectric hysteresis loops were measured using a conventional Sawyer–Tower circuit in order to apply an electric field with a triangular waveform. The electric field-induced strain was measured using a linear variable differential transducer (LVDT, Mitutoyo MCH-331 & M401). The voltage was supplied by a high voltage amplifier (Trek, 610E) driven by a waveform generator (Agilent 33250A). The normalized strain ($d^*_{33} = S_{max}/E_{max}$) was calculated as the ratio of the maximum strain to the maximum electric field observed in the unipolar strain-field curves.

3. Results and discussion

Fig. 1(a) shows the X-ray diffraction patterns of the BNKT–BA ceramics in the 2θ range of 20–60°. Each of the ceramics possessed a pure perovskite phase and no secondary phase was detected. The absence of secondary phases indicates that the K^+ and Al^{3+} ions successfully diffused into the BNT lattice to form a homogeneous solid solution. Fig. 1(b) illustrates the detailed XRD analysis in the 2θ range of 39–48°. It is known that BNT and BA are rhombohedral while BKT is tetragonal at room temperature [12–14,19]. The rhombohedral symmetry of BNT is characterized by the splitting of the (0 0 3)/(0 2 1) peaks around a 2θ of 40° and a single (2 0 2) peak around a 2θ of 46.5°. The crystal structure of BKT with tetragonal symmetry is characterized by the splitting of the (0 0 2)/(2 0 0) peaks around a 2θ of 46.5° and the existence of a single (1 1 1) peak at a 2θ of approximately 40°. In Fig. 1(b), the distinct splitting of the (0 0 2)/(2 0 0) peaks at a 2θ of 46.5° can be seen when $x \geq 0.15$, corresponding to a tetragonal symmetry. The (0 0 3)/(0 2 1) peak splitting at approximately a 2θ of 40° was obvious up to $x = 0.20$. Therefore, it can be suggested that the MPB of the BNKT–BA system existed in the composition range of $0.15 \leq x \leq 0.20$ at room temperature, where rhombohedral and tetragonal phases coexisted. In addition, as the K^+ fraction in the solid solution was increased, the diffraction peaks of the BNKT–BA ceramics shifted slightly to lower 2θ angles, indicating an increase of the lattice constant as the K^+ content increased. Furthermore, an increase in the K^+ fraction intensified the separation of the (0 0 2)/(2 0 0) peaks, suggesting an increase in the tetragonality of the lattice. As an example of the peak shifts, the 2θ angles of the diffraction peak around 46° for all of the BNKT–BA ceramics are shown in Fig. 2. The corresponding space distance (d) calculated using Bragg's equation, $2d \sin\theta = \lambda$ ($\lambda = 1.5418$ Å for Cu $K\alpha$ radiation), is also shown in Fig. 2. The value of d_{202} for the BNKT–BA ceramics at $x = 0$ is about 1.944 Å, which increased slightly with the addition of K^+ content, corresponding to a decrease of the 2θ angle values. As the ionic radius of K^+ (1.33 Å) is much larger than that of Na^+ (0.97 Å), the substitution of K^+ for Na^+ could result in expansion of the BNT crystals

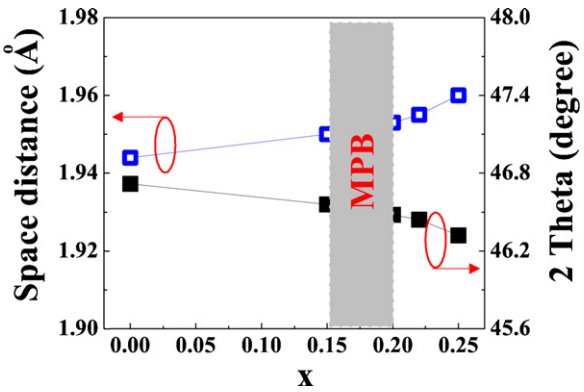

Fig. 2. The relationships between the space distance and 2θ with the K content in the BNKT–BA ceramics.

[26,27]. It is noted that a transition in the different peaks or the space distance was observed at 20 mol% K^+ content as the value of d_{202} for BNKT–BA with $x = 0$ linearly increased as the K^+ content increased to 20 mol%. Then, d for the BNKT–BA phase linearly increased to the d_{200} of BNKT–BA as the K^+ content increased from 20 to 25 mol%. These results suggest the possibility of the existence of a MPB-like region in the BNKT–BA system located in the K^+ composition range of 15–20 mol%. It is worth noting that the position of the MPB observed in our BNKT–BA ceramics was slightly different from those previously reported studies for BNT–BKT [12–14], in which the MPB was located in the range from 16 to 20 mol% K^+. The reasons for this discrepancy are not clear. However, there may be two possibilities for this slight shift of MPB from 16 mol% K^+ to 15 mol% K^+. Firstly, the composition 15 mol% K^+ is very close to the MPB region, which has a possibility to show MPB behavior because all of the reported studies ignored this composition [12–14]. Secondly, this slight MPB composition shift from 16 to 15 mol% K^+ is acceptable, particularly when considering the multiplying effects of $BiAlO_3$ (2.5 mol%).

Fig. 3 shows SEM micrographs of the polished and thermally etched BNKT–BA ceramic samples. The SEM observations confirmed that all samples were dense with a well developed microstructure. The substitution of K^+ for Na^+ led to an obvious change in the grain shape and size. For BNKT–BA ceramics with $x = 0.15$, the grains had diameters in the range of 1.5–2 μm (Fig. 3(a)). As the substitution level of K^+ increased from 0.15 to 0.25, the grains became significantly smaller (0.7–1 μm) and grew into neat rectangular and cubic shapes (Fig. 3(d)). This indicates that an increase of the K^+ concentration suppressed the grain growth rate of the ceramics and promoted the formation of grains with a cubic shape. This is because K^+ ions concentrate near grain boundaries and their mobility decreases substantially as densification occurs. The reduction in the mobility of the grain boundary weakens the mass transport. As a result, grain growth was slightly inhibited and smaller grains were formed in the BNKT–BA ceramics at high concentrations of K^+. The effect of K^+ on the grain growth in the BNKT–BA ceramics is similar to that in BNT–$Bi_{0.5}K_{0.5}TiO_3$ [13,28], BNT–$Bi_{0.5}K_{0.5}TiO_3$–$BaTiO_3$ [29], and BNT–$Bi_{0.5}K_{0.5}TiO_3$–$Bi_{0.5}Li_{0.5}TiO_3$ ceramics [30].

Fig. 4 shows the temperature-dependences of the dielectric constant and the dielectric losses of poled BNKT–BA ceramics at frequencies of 1, 10, 50, and 100 kHz. It has been reported that BNT and BNT-based ceramics exhibit two dielectric anomalies corresponding to the maximum dielectric constant temperature (T_m) and depolarization temperature (T_d) [5,6,29,30]. From Fig. 4(a), ceramics with $x = 0$ showed only the high dielectric anomaly at T_m, while the dielectric anomaly at T_d was not apparent. On the other hand, the dielectric curves of the ceramics with $x = 0.15$ exhibited a sharp T_d peak and the dielectric anomaly at T_m was relatively broad. A further increase in the K^+ concentration gradually broadened the dielectric anomalies at T_m and T_d, suggesting that the K^+ concentration induced a diffuse phase transition in the BNKT–BA ceramics.

It is widely known that dielectric properties are related to the phase structure and domain alignment. In the BNKT–BA ceramics, the dielectric constant at T_m significantly increased with increasing K^+ content, reached a maximum value of 6269 (at 1 kHz) at $x = 0.20$ and then decreasing. Near the MPB composition (i.e., $x = 0.20$), the crystal structure included both the rhombohedral and tetragonal phases. The free energy of the rhombohedral phase is

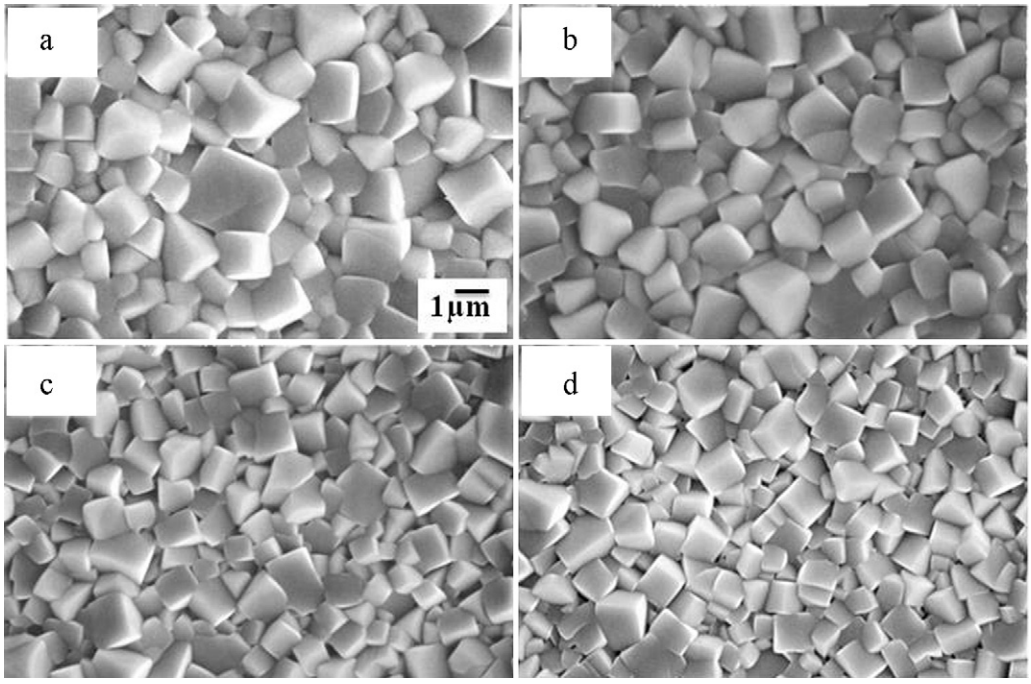

Fig. 3. SEM micrographs of the BNKT–BA ceramics with various K contents: (a) $x = 0.15$, (b) $x = 0.20$, (c) $x = 0.22$, and (d) $x = 0.25$.

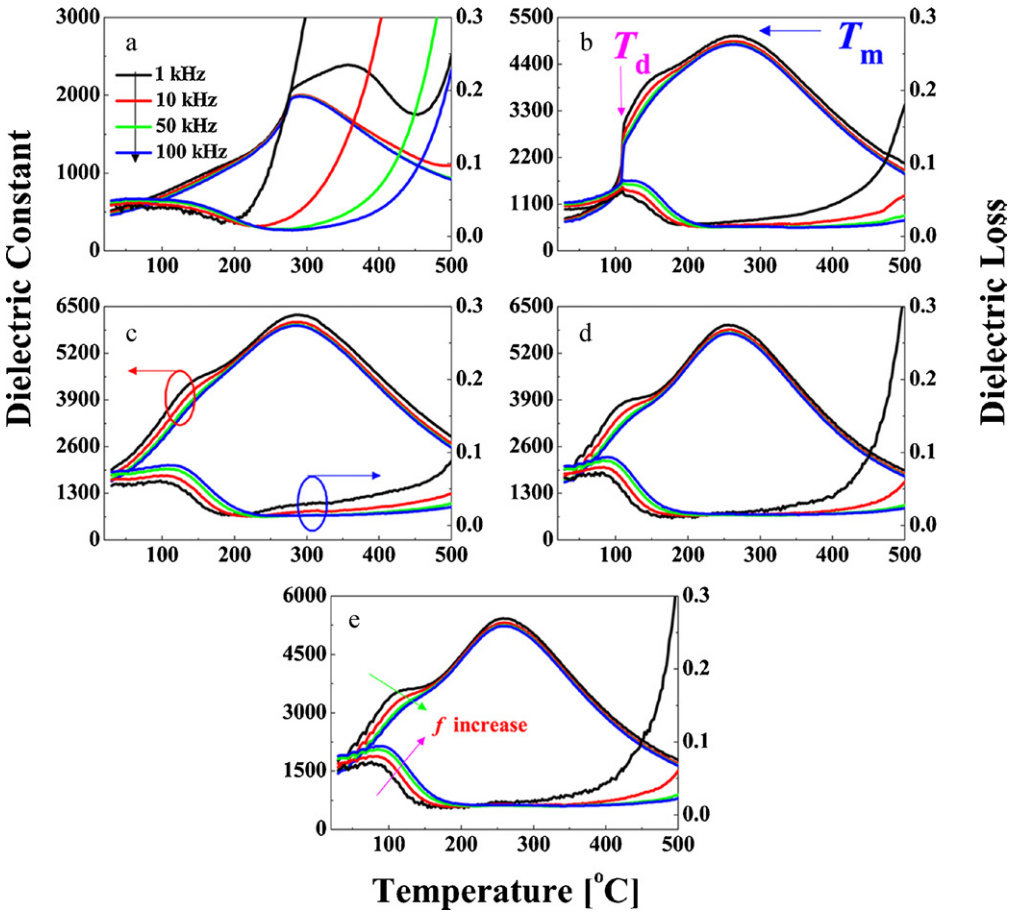

Fig. 4. Dielectric constants and dielectric losses of the BNKT–BA ceramics as a function of temperature and frequency: (a) $x = 0$, (b) $x = 0.15$, (c) $x = 0.20$, (d) $x = 0.22$, and (e) $x = 0.25$.

similar to that of the tetragonal phase. Movement and polarization of the ferroelectric active ions were promoted in this case, leading to the increase of the dielectric constant. The dielectric loss of the ceramics increased somewhat with increasing K^+ content and varied between 0.04 and 0.07. Moreover, the depolarization temperature (T_d) and maximum dielectric constant temperature (T_m) decreased as potassium was substituted for sodium. Generally, the MPB composition (coexistence of rhombohedral and tetragonal phases) in the BNT–BKT system has a lower depolarization temperature (T_d) than the rhombohedral and tetragonal phases [16,31]. However, in BNKT–BA ceramics, the continuous decrease of T_d may be due to the possible existence of non-polar regions induced by the higher K^+ content ($x \geq 0.20$), which is evident from the slightly pinched shape of the *P*–*E* hysteresis loops shown in Fig. 5. Zheng et al. [32] observed similar behavior in $(Bi_{0.94-x}La_xNa_{0.94})_{0.5}Ba_{0.06}TiO_3$ ceramics, in which T_d decreased due to the substitution of La^{3+} for Bi^{3+} because of the existence of non-polar regions.

Fig. 5 shows the *P*–*E* hysteresis loops of the BNKT–BA ceramics measured at room temperature. Ceramics without the addition of K^+ exhibited a roughly square *P*–*E* hysteresis loop with a remanent polarization and maximum polarization of 15 μC/cm^2 and 18 μC/cm^2, respectively, and a coercive field of 47 kV/cm. The remanent polarization (P_r), maximum polarization (P_m), and coercive field (E_c) of the BNKT–BA ceramics as a function of the K^+ content are shown in Fig. 6. The remanent polarization increased considerably with increasing K^+ content and reached its maximum at $x = 0.15$ near the rhombohedral side of the MPB composition. The tetragonal phase has six different polarizations in the ⟨0 0 1⟩ direction for reorientation, while there are eight different ⟨1 1 1⟩ directions in the rhombohedral phase [33]. Therefore, both of these phases may coexist with compositions near the MPB to produce 14 possible polarization directions. The large number of polarization directions cause enhanced crystallographic orientations under the electric field and, in turn, result in high polarization and piezoelectric properties. In the present work, the maximum remanent polarization of 25 μC/cm^2 was obtained on the rhombohedral side of the MPB composition ($x = 0.15$), primarily due to the rhombohedral phase having a more reoriented direction compared to that of the tetragonal phase. Therefore, the rhombohedral phase could achieve a larger remanent polarization. Furthermore, an increase in the K^+ concentration ($x \geq 0.20$) led to an obvious change in the loop shapes and polarization values. The remanent polarization decreased from 25 μC/cm^2 to 18 μC/cm^2 and the coercive field dropped steeply from 40 kV/cm to 13 kV/cm as x was increased from 0.15 to 0.20, resulting in slightly pinched and narrow *P*–*E* hysteresis loops. Conversely, the maximum polarization, P_m, was unaffected. The drastic decreases in the coercive field and remanent polarization accompanied by slightly pinched *P*–*E* hysteresis loops may be attributed to the existence of a non-polar phase induced by the higher K^+ content ($x \geq 0.20$). Similar results have been reported in $(Bi_{0.5}Na_{0.5})_{0.94}Ba_{0.06}Zr_yTi_{1-y}O_3$ [34], $(Bi_{0.92}Na_{0.92-x}Li_x)_{0.5}Ba_{0.06}Sr_{0.02}TiO_3$ [35], BNT–$KNbO_3$ [36], and BNT–$SrTiO_3$ ceramics [37]. The substitutions of Zr^{4+} for Ti^{4+} in the 0.94BNT–0.06$BaTiO_3$, Li^+ for Na^+ in BNT–BST, and the introduction of $KNbO_3$ or $SrTiO_3$ into BNT shift the depolarization temperature, T_d, towards room temperature, leading to the appearance of the non-polar phase. The interaction between the polar and non-polar

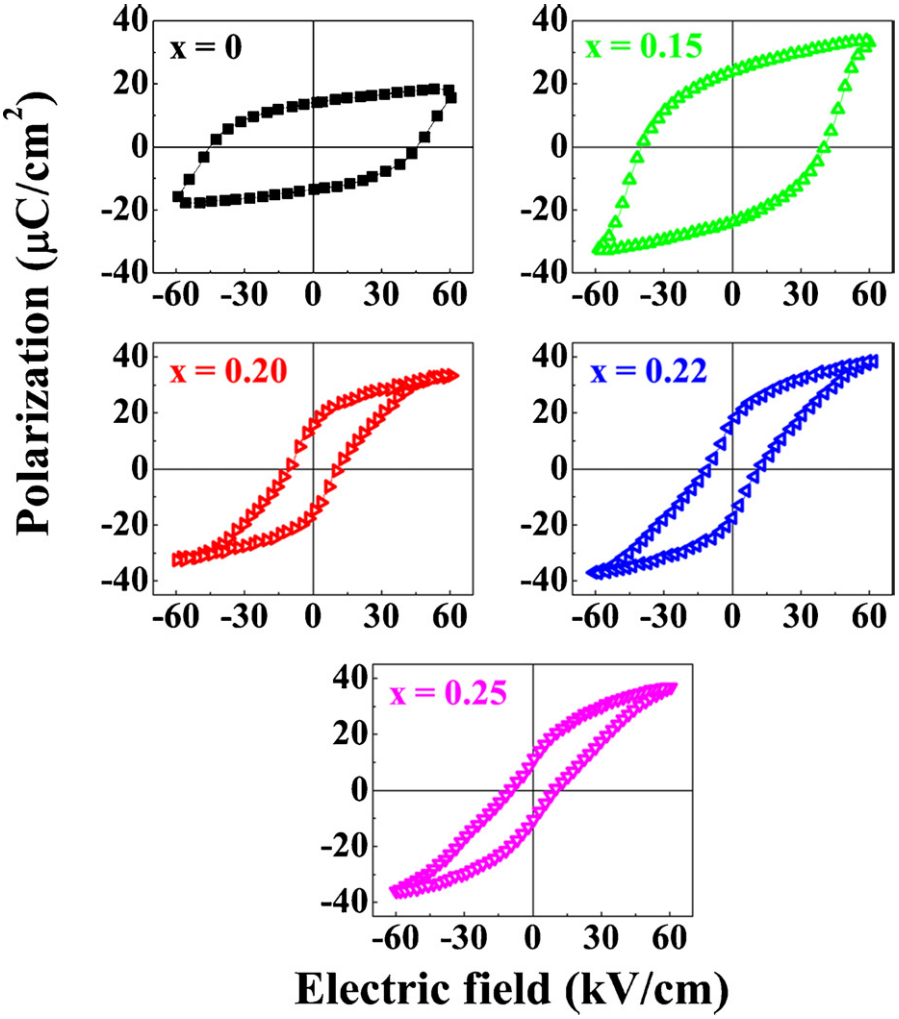

Fig. 5. Polarization hysteresis loops of the BNKT–BA ceramics with a maximum field of 60 kV/cm at room temperature.

phases gives rise to the deformation of the *P*–*E* hysteresis loop [34–37].

Fig. 7(a) shows the bipolar electric field-induced strain curves of the BNKT–BA ceramics measured at room temperature. The "*negative strain*", which denotes the difference between the zero field strain and the lowest strain and is only visible in the bipolar cycle [38], is summarized as a function of the K^+ content in Fig. 7(b).

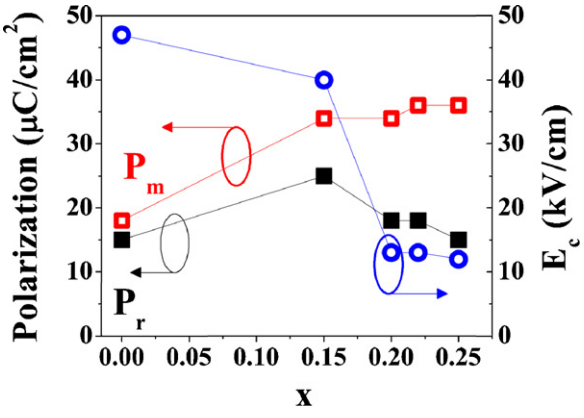

Fig. 6. Maximum polarization (P_m), remanent polarization (P_r), and coercive field (E_c) of the BNKT–BA ceramics as a function of the K content.

The shape of the strain curve can be separated into three parts: the rhombohedral phase, the broad MPB composition range, and the tetragonal phase. It is evident from Fig. 7(a) that the rhombohedral phase of the BNKT–BA ceramics produced the smallest strain. The maximum strain and negative strain increased significantly when the BNKT–BA composition moved from the rhombohedral phase to the MPB. The tetragonal side of the MPB composition ($x = 0.20$) demonstrated nearly equal values of maximum strain and negative strain of ~0.16% and −0.14%, respectively, and displayed a well defined typical butterfly *S*–*E* loop. However, when the symmetry changed to the tetragonal phase ($x = 0.22$), the maximum strain increased abruptly to 0.33%, which is about twice that at $x = 0.20$, which was located at the tetragonal boundary of the MPB. Conversely, the negative strain, which is closely related to domain back switching during bipolar cycles, sharply decreased to −0.07%, about half of its value at the tetragonal boundary of the MPB ($x = 0.20$). Beyond $x = 0.22$, the maximum strain decreased slightly to 0.29% while the negative strain decreased drastically to −0.012%. As a result, the strain curve exhibited a drastic deviation from the butterfly *S*–*E* loops. It should be noted that at $x \geq 0.22$, the samples possessed tetragonal symmetry. However, the significant reduction of the negative strain accompanied by the deviation from the butterfly *S*–*E* loops again revealed that the ferroelectric and non-polar phases coexisted at these compositions and that an easy transition between the ferroelectric and non-polar phases occurred under an electric field due to its comparable free energy, resulting in the

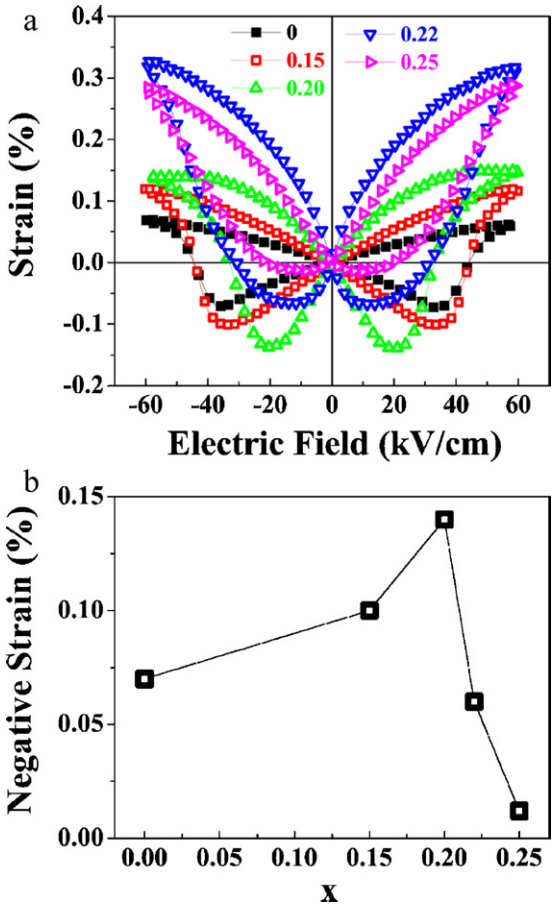

Fig. 7. (a) Bipolar strain hysteresis loops of the BNKT–BA ($x = 0$, 0.15, 0.20, 0.22, and 0.25) ceramics and (b) negative strain (%) as a function of the K content in the BNKT–BA ceramics.

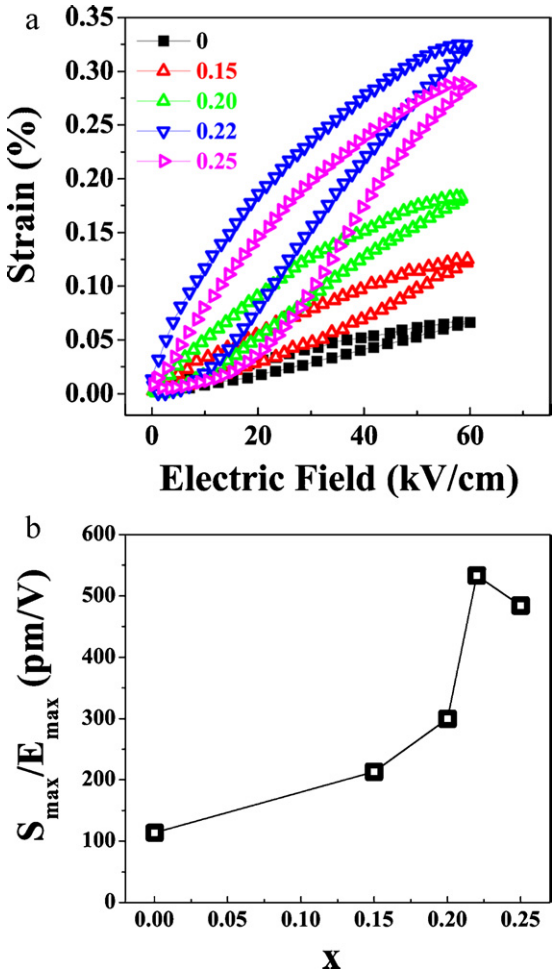

Fig. 8. (a) Unipolar strain hysteresis loops of the BNKT–BA ($x = 0$, 0.15, 0.20, 0.22, and 0.25) ceramics and (b) the normalized strain (S_{max}/E_{max}) as a function of the K content in the BNKT–BA ceramics.

large strain. The behaviors of the bipolar *S*–*E* loops were in good agreement with the ferroelectric behaviors shown in Fig. 5, where the slightly pinched hysteresis loops and the destabilization of the ferroelectric order at high concentrations of K^+ ($x \geq 0.22$) may indicate that different polarization states (ferroelectric and non-polar) coexisted at these compositions. Similar large electric field-induced strains have been reported in Zr-modified $Bi_{0.5}(Na_{0.78}K_{0.22})_{0.5}TiO_3$ ceramics in which the substitution of 3 mol% Zr^{4+} for Ti^{4+} disrupts the ferroelectric phase of $Bi_{0.5}(Na_{0.78}K_{0.22})_{0.5}TiO_3$ ceramics, leading to the existence of a non-polar phase [39]. Even so, no crystal structure variations have been reported and the symmetry was tetragonal in the studied composition range. Based on electrical measurements, a field-induced ferroelectric to non-polar phase transition has been suggested to cause the reported large strains. In a recent report from Seifert et al. [40], a large strain was observed in $(Bi_{1/2}Na_{1/2})TiO_3$–$(Bi_{1/2}K_{1/2})TiO_3$–$(K_{0.5}Na_{0.5})NbO_3$ ceramics. The researchers found that the ferroelectric order of BNT–BKT was significantly disrupted by the replacement of KNN for BNT, leading to a significant reduction of the remanent polarization and negative strain. However, the destabilization of the ferroelectric order was accompanied by a significant enhancement in the strain behavior.

Fig. 8(a) shows the unipolar electric field-induced strain curves of the BNKT–BA ceramics measured at 60 kV/cm. Similar to the bipolar strain, the unipolar strain also increased with increasing K^+ content up $x = 0.22$, beyond which it decreased slightly with increasing K^+ concentration. The normalized strains ($d^*_{33} = S_{max}/E_{max}$) of the BNKT–BA ceramics as a function of K^+ content are depicted in Fig. 8(b), and were calculated as the ratio of the maximum strain (S_{max}) to the maximum electric field (E_{max}) [38]. A large strain ($S = 0.33\%$) and corresponding normalized strain ($d^*_{33} = 533$ pm/V) were obtained at $x = 0.22$, which are comparable to those of previously reported lead-free BNT-based materials [23,37,38], suggesting promise for lead-free electromechanical applications.

In general, the electric field-induced strain in ceramics is caused by complicated domain switching, piezoelectricity, and the electric field [2,41]. In other words, the strain value is dependent on domain switching, the piezoelectric constant, polarization, and the applied electric field. In our study, the strain was maximized at the tetragonal symmetry composition ($x = 0.22$). Therefore, this large strain was not caused solely by the polarization, but also by the coexistence of phases in the applied electric field because the remanent polarization at $x = 0.22$ was lower than that at the MPB composition (Fig. 6) and the bipolar strain curve deviated from that of typical ferroelectric materials (Fig. 7). This phenomenon is similar to those observed in $Bi_{0.5}(Na_{0.78}K_{0.22})_{0.5}(Ti_{1-x}Zr_x)O_3$ [39], BNT–BKT–KNN [40], and BNT–BT–KNN ceramic systems [42]. In agreement with other reports [39,40,42], the coexistence of different polarization states in the present study may also indicate that the free energy of the ferroelectric phase is competitive with that of the non-polar phase. The field-induced strain caused by the ferroelectric non-polar phase transition was larger than that caused solely by ferroelectric domain switching. Therefore, on the basis of the *P*–*E* hysteresis loops and the *S*–*E* loops, our results suggest that this large electric field-induced strain was caused by mixed contributions of ferroelectric and non-polar phases.

4. Conclusions

Lead-free piezoelectric ceramics, $0.975[Bi_{0.5}(Na_{1-x}K_x)_{0.5}TiO_3]$ $-0.025BiAlO_3$, were successfully synthesized using a solid state reaction method and the effects of potassium concentration on their structures and electrical properties were studied in detail. Increases in the K^+ concentration decreased the grain growth rate and changed the grain morphologies to cubic shapes. A morphotropic phase boundary (MPB) was identified in the BNKT–BA ceramics with K^+ contents of $0.15 \leq x \leq 0.20$. The BNKT–BA composition near the rhombohedral side of the MPB ($x = 0.15$) possessed a higher remanent polarization of 25 $\mu C/cm^2$ and a coercive field of 40 kV/cm while the composition near the tetragonal side of the MPB ($x = 0.20$) had a higher dielectric constant. The electric field-induced strain and the corresponding normalized strain, d^*_{33}, increased dramatically when the composition moved from the MPB to the tetragonal phase. In particular, a very large electric field-induced strain ($S = 0.33\%$) and a corresponding normalized strain ($d^*_{33} = 533$ pm/V) were obtained on the tetragonal side ($x = 0.22$) close to the MPB. This value of d^*_{33} indicates that BNKT–BA ceramics are candidate materials for lead-free electromechanical applications.

Acknowledgements

This research was financially supported by the Ministry of Education, Science and Technology (MEST) and the Korea Institute for the Advancement of Technology (KIAT) through the Human Resource Training Project for Regional Innovation. The authors also acknowledge the Priority Research Centers Program through the National Research Foundation of Korea (NRF) funded by the Ministry of Education, Science and Technology (2009-0093818).

References

[1] G.H. Haertling, J. Am. Ceram. Soc. 82 (1999) 797–818.
[2] S.E. Park, T.R. Shrout, J. Appl. Phys. 82 (1997) 1804–1811.
[3] Y. Li, K.S. Moon, C.P. Wong, Science 308 (2005) 1419–1420.
[4] L.E. Cross, Nature 432 (2004) 24–25.
[5] G.A. Smolenskii, V.A. Isupov, A.I. Agranovskaya, N.N. Krainik, Sov. Phys. Solid State (Engl. Transl.) 2 (1961) 2651–2654.
[6] T. Takenaka, K. Maruyama, K. Sakata, Jpn. J. Appl. Phys. 30 (1991) 2236–2239.
[7] M. Cernea, E. Andronescu, R. Radu, F. Fochi, C. Galassi, J. Alloys Compd. 490 (2010) 690–694.
[8] H. Ishii, H. Nagata, T. Takenaka, Jpn. J. Appl. Phys. 40 (2001) 5660–5663.
[9] W.C. Lee, C.Y. Huang, L.K. Tsao, Y.C. Wu, J. Alloys Compd. 492 (2010) 307–312.
[10] W. Krauss, D. Schutz, F.A. Mautner, A. Feteira, K. Reichmann, J. Eur. Ceram. Soc. 30 (2010) 1827–1832.
[11] D. Lin, K.W. Kwok, H.L.W. Chan, J. Alloys Compd. 481 (2009) 310–315.
[12] A. Sasaki, T. Chiba, Y. Mamiya, E. Otsuki, Jpn. J. Appl. Phys. 38 (1999) 5564–5567.
[13] Z. Yang, B. Liu, L. Wei, Y. Hou, Mater. Res. Bull. 43 (2008) 81–89.
[14] W. Zhao, H. Zhou, Y. Yan, D. Liu, Key Eng. Mater. 368–372 (2008) 1908–1910.
[15] X. Chen, Y. Liao, H. Wang, L. Mao, D. Xiao, J. Zhu, Q. Chen, J. Alloys Compd. 493 (2010) 368–371.
[16] K. Yoshii, Y. Hiruma, H. Nagatha, T. Takenaka, Jpn. J. Appl. Phys. 45 (2006) 4493–4496.
[17] M. Zou, H. Fan, L. Chen, W. Yang, J. Alloys Compd. 495 (2010) 280–283.
[18] X. Chen, X. Gong, T. Li, Y. He, P. Liu, J. Alloys Compd. 507 (2010) 535–541.
[19] P. Baettig, C.F. Schelle, R. LeSar, U.V. Waghmare, N.A. Spaldin, Chem. Mater. 17 (2005) 1376–1380.
[20] J. Zylberberg, A.A. Belik, E. Takayama-Muromachi, Z.-G. Ye, Chem. Mater. 19 (2007) 6385–6390.
[21] Y. Watanaba, Y. Hiruma, H. Nagata, T. Takenaka, Key Eng. Mater. 388 (2009) 229–232.
[22] H. Yu, Z.-G. Ye, Appl. Phys. Lett. 93 (2008), 112902.
[23] Y. Hiruma, H. Nagata, T. Takenaka, Jpn. J. Appl. Phys. 48 (2009), 09KC08.
[24] A. Ullah, C.W. Ahn, K.B. Jang, A. Hussain, I.W. Kim, Ferroelectrics 404 (2010) 167–172.
[25] A. Ullah, S.Y. Lee, H.J. Lee, I.W. Kim, C.W. Ahn, H.-I. Hwang, A. Hussain, J.S. Lee, J. Korean Phys. Soc. 57 (2010) 1102–1105.
[26] Y.R. Zhang, J.F. Li, B.P. Zhang, C.E. Peng, J. Appl. Phys. 103 (2008), 074109.
[27] B.P. Zhang, J.F. Li, K. Wang, H. Zhang, J. Am. Ceram. Soc. 89 (2006) 1605–1609.
[28] E. Fukuchi, T. Kimura, T. Tani, T. Takeuch, Y. Saito, J. Am. Ceram. Soc. 85 (6) (2002) 1461–1466.
[29] X.X. Wang, S.H. Choy, X.G. Tang, H.L.W. Chan, J. Appl. Phys. 97 (2005), 104101.
[30] D. Lin, Q. Zheng, C. Xu, K.W. Kwok, Appl. Phys. A 93 (2008) 549–558.
[31] T. Takenaka, H. Nagata, Y. Hiruma, IEEE Trans. Ultrason. Ferroelect. Freq. Contr. 56 (2009) 1595–1612.
[32] Q. Zheng, C. Xu, D. Lin, D. Gao, K.W. Kwok, J. Phys. D: Appl. Phys. 41 (2008), 125411.
[33] C.A. Randall, N. Kim, J. Kucera, W. Cao, T.R. Shrout, J. Am. Ceram. Soc. 81 (1998) 677–688.
[34] Y.Q. Yao, T.Y. Tseng, C.C. Chou, H.H.D. Chen, J. Appl. Phys. 102 (2007), 094102.
[35] D. Lin, K.W. Kwok, Curr. Appl. Phys. 10 (2010) 1196–1202.
[36] G. Fan, W. Lu, X. Wang, F. Liang, J. Xiao, J. Phys. D: Appl. Phys. 41 (2008), 035403.
[37] Y. Hiruma, Y.O. Imai, Y. Watanabe, H. Nagata, T. Takenaka, Appl. Phys. Lett. 92 (2008), 262904.
[38] S.-T. Zhang, A.B. Kounga, E. Aulbach, T. Granzow, W. Jo, H.-J. Kleebe, J. Rodel, J. Appl. Phys. 103 (2008), 034107.
[39] A. Hussain, C.W. Ahn, J.S. Lee, A. Ullah, I.W. Kim, Sens. Actuators A: Phys. 158 (2010) 84–89.
[40] K.T.P. Seifert, W. Jo, J. Rodel, J. Am. Ceram. Soc. 93 (2010) 1392–1396.
[41] Y. Masuda, Jpn. J. Appl. Phys. 33 (1994) 5549–5554.
[42] W. Jo, T. Granzow, E. Aulbach, J. Rodel, D. Damjanovic, J. Appl. Phys. 105 (2009), 094102.